^{5}CpFe(2,5-Dimethylpyrrolid) (18)

ESI-MS

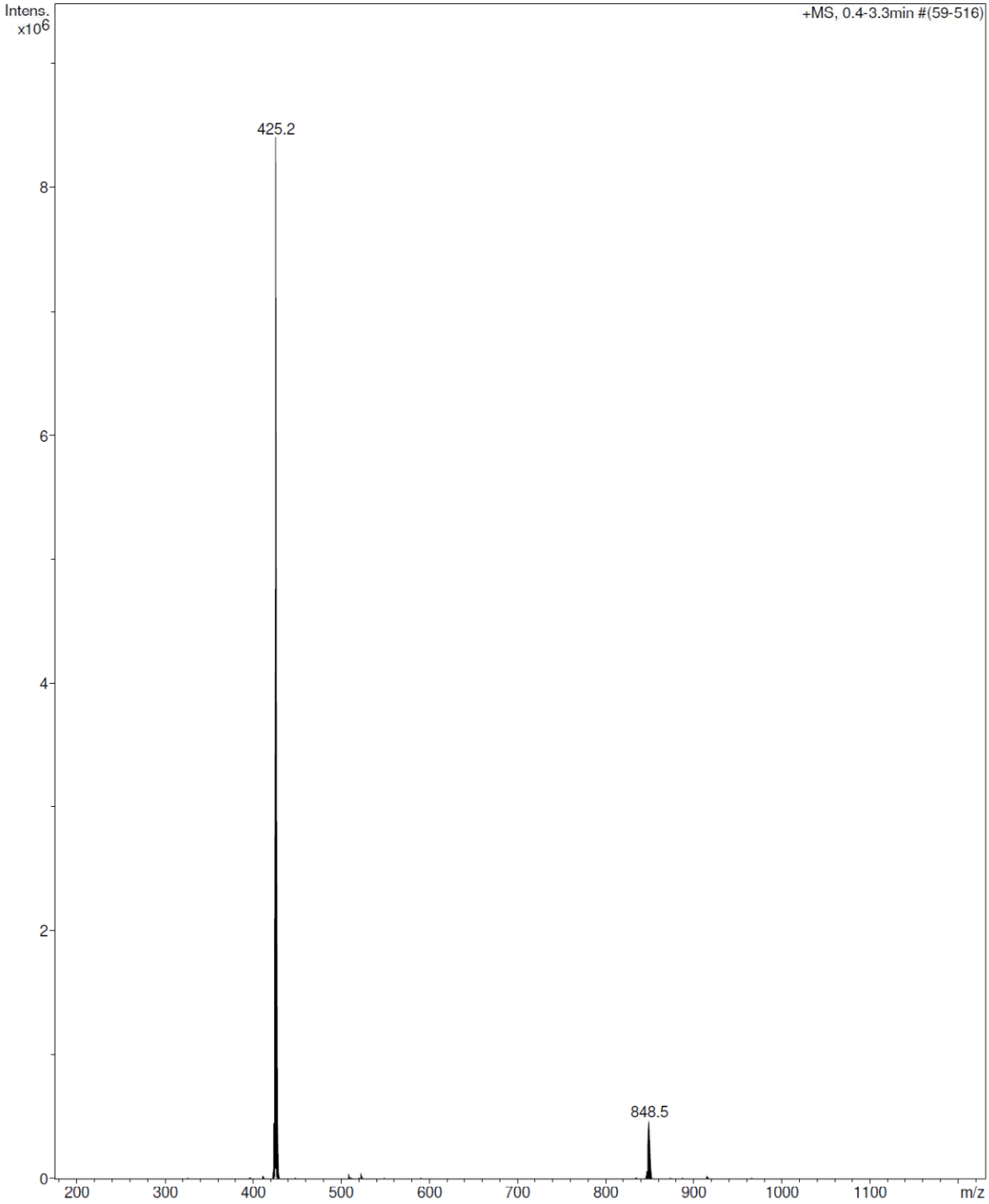

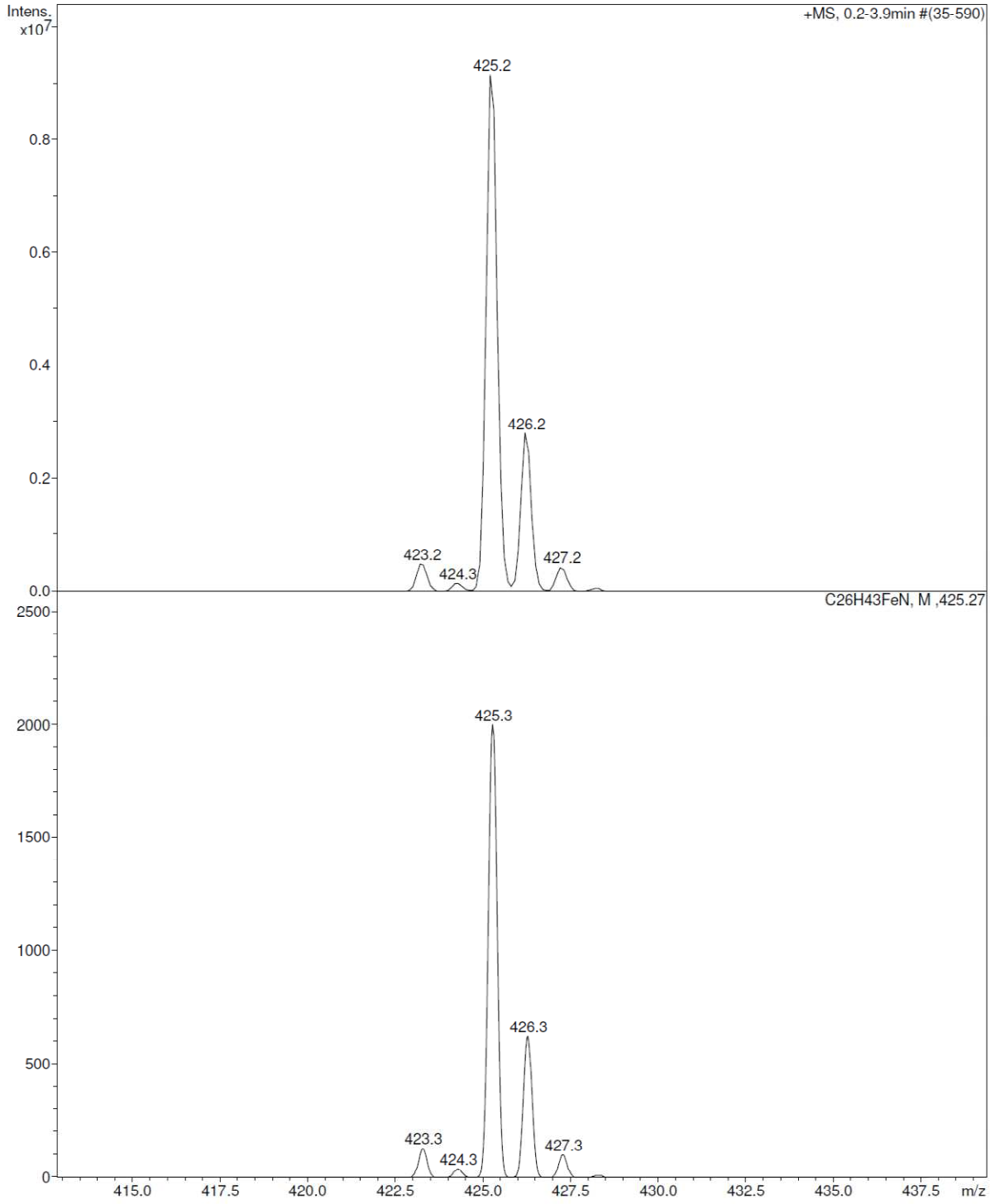
Intens.
x10^7
+MS, 0.2-3.9min #(35-590)
425.2
426.2
423.2
424.3
427.2
C26H43FeN, M ,425.27
425.3
426.3
423.3
424.3
427.3
m/z

^{1}H-NMR

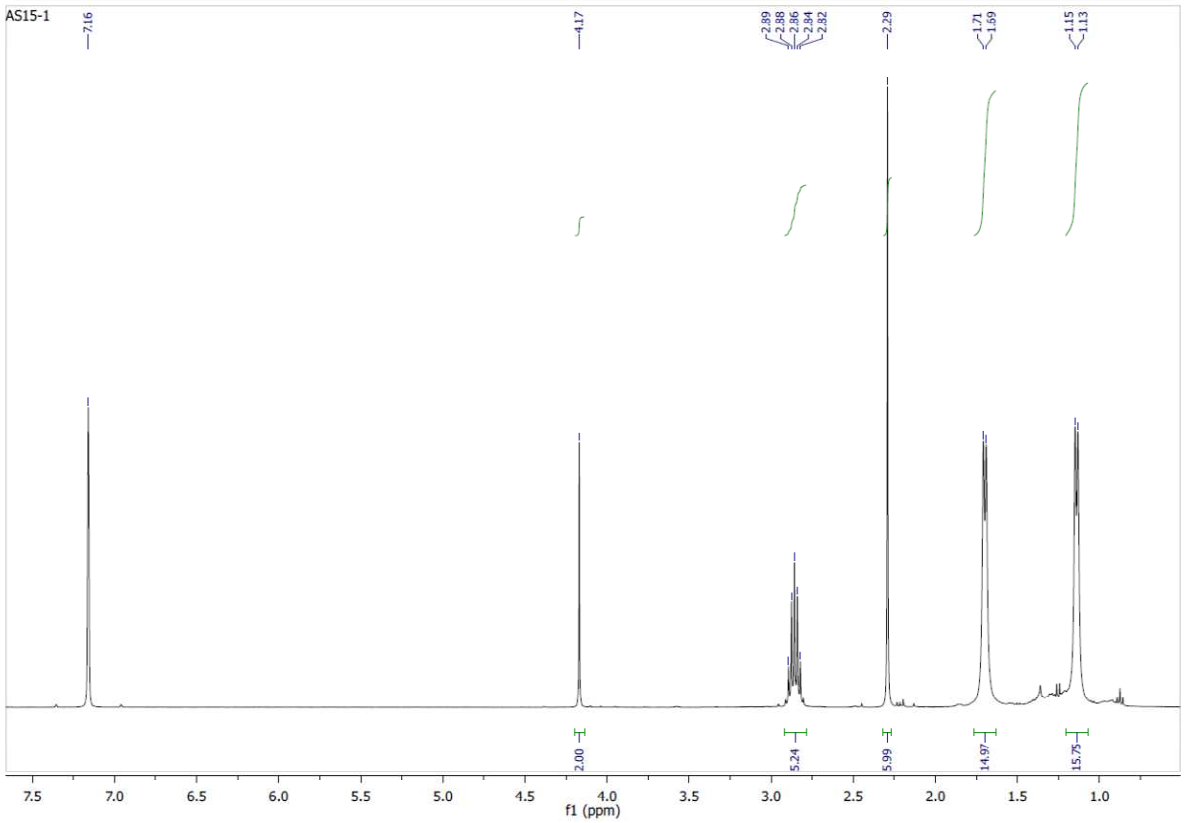

^{13}C-NMR

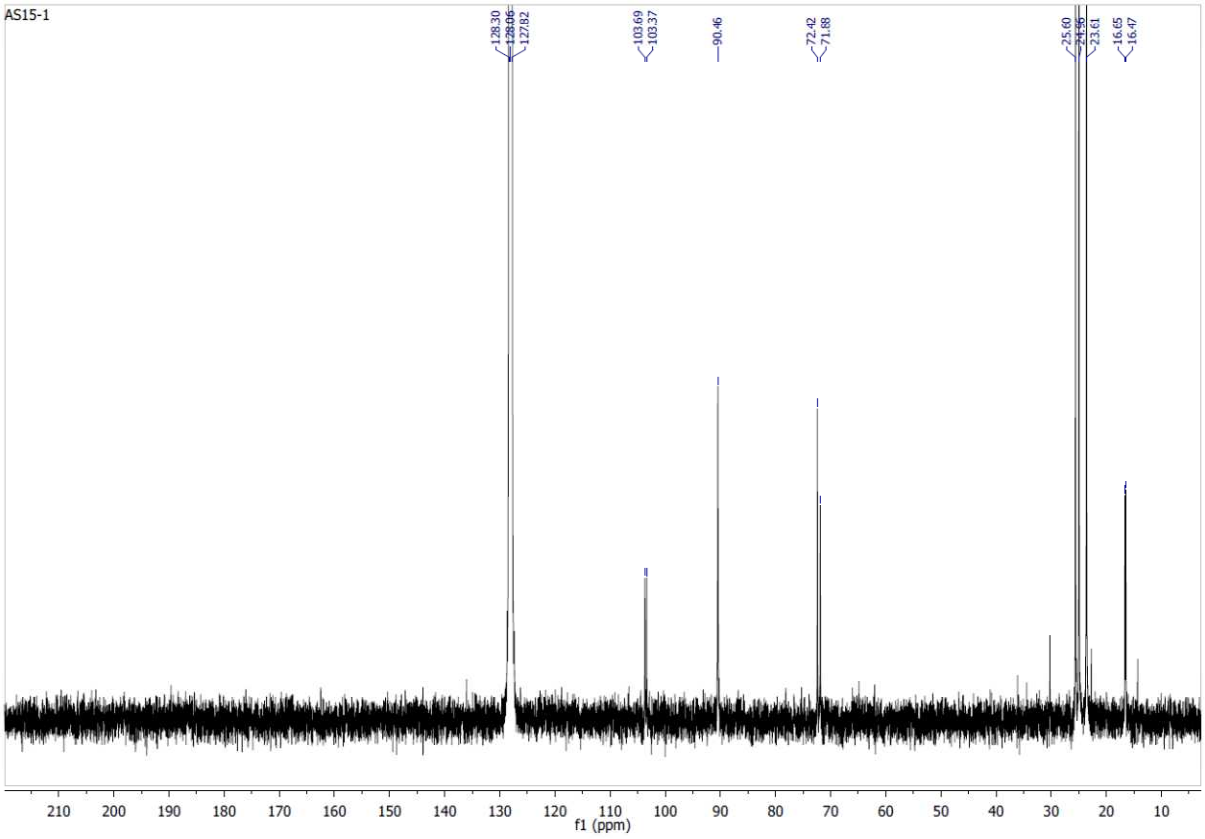

$(^5CpFe(OH))_2$ (21)

^{1}H-NMR

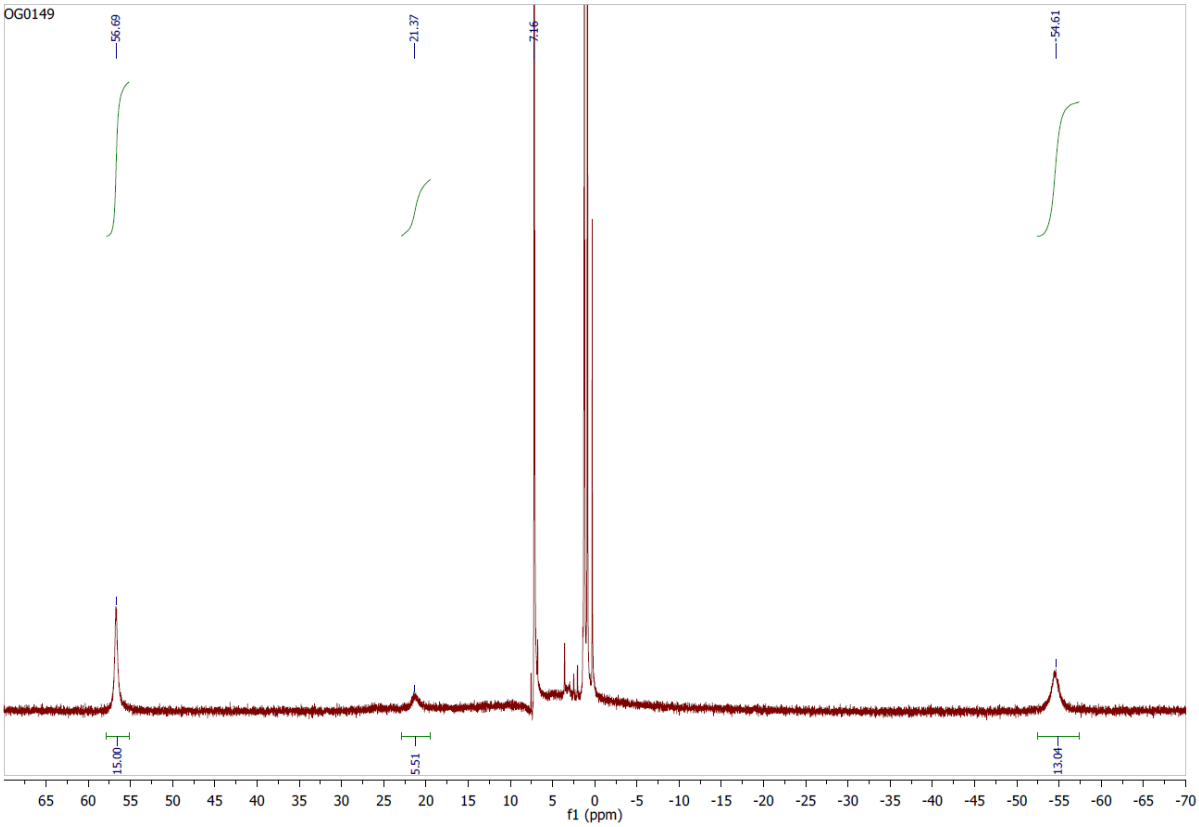

$(^5CpFe)_2$ (8)

^{1}H-NMR

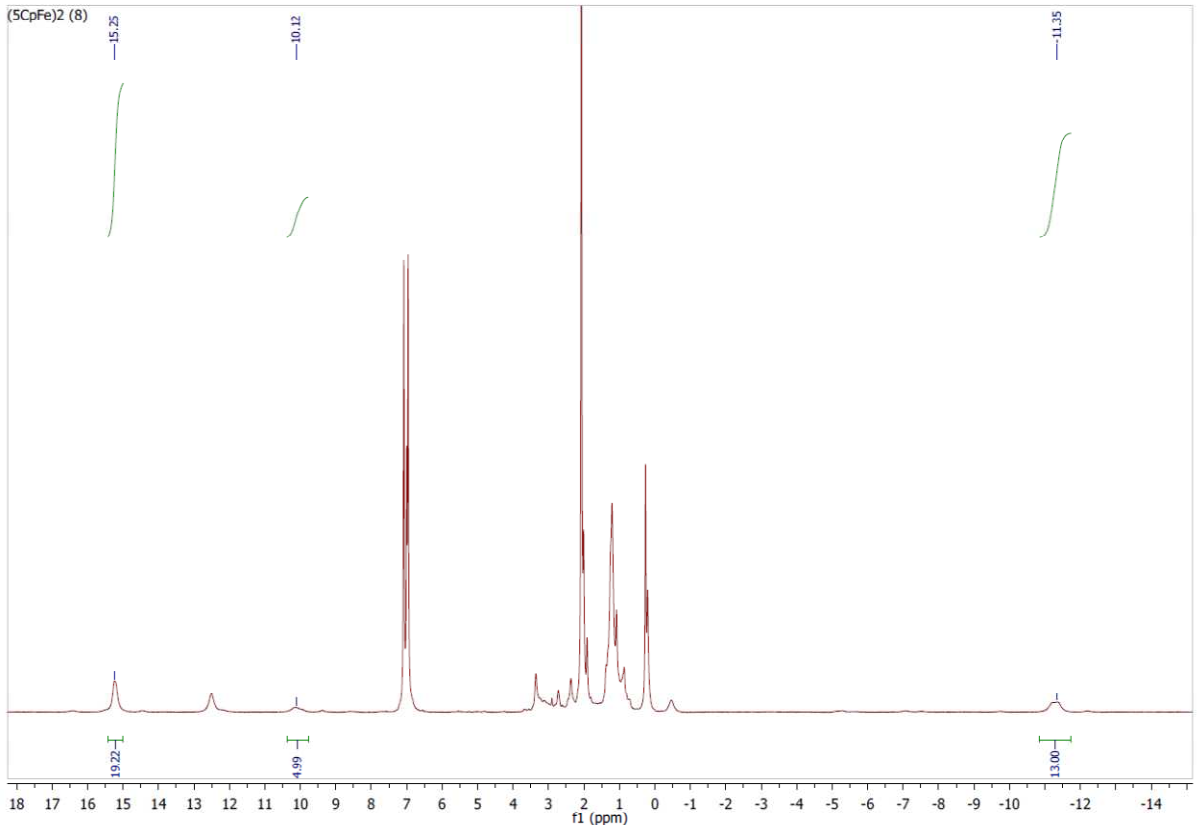

XANES

Experimental details:

XAS experiments were performed at the SPLINE-beamline BM25A of the ESRF (European Synchrotron Radiation Facility) in Grenoble (France). The measurement at the iron K-edge at 7.112 keV was carried out with a Si(311) double-crystal monochromator and a maximum synchrotron beam current of 200 mA. Spectra were recorded in transmission mode and in solid form diluted with cellulose. The preparation of the sample was carried out under inert atmosphere in a glove box. For energy calibration iron foil was used.

X-ray absorption spectroscopy provides the opportunity to gain with one method manifold information about a substance. Analysis of the energy shift and the shape of the absorption edge, the so-called X-ray absorption near edge structure (XANES), yields the oxidation state and the geometric coordination of the absorbing atom. The XAS spectrum of $^5Cp_2Fe_2$ is plotted in figure 1. To determine the oxidation state of iron in the complex two reference materials, an iron foil (Fe^0) and ferrocene (Fe^{+II}) are shown for comparison. To illustrate small distinctions, the first derivatives of the absorption spectra are shown in figure 1, too.

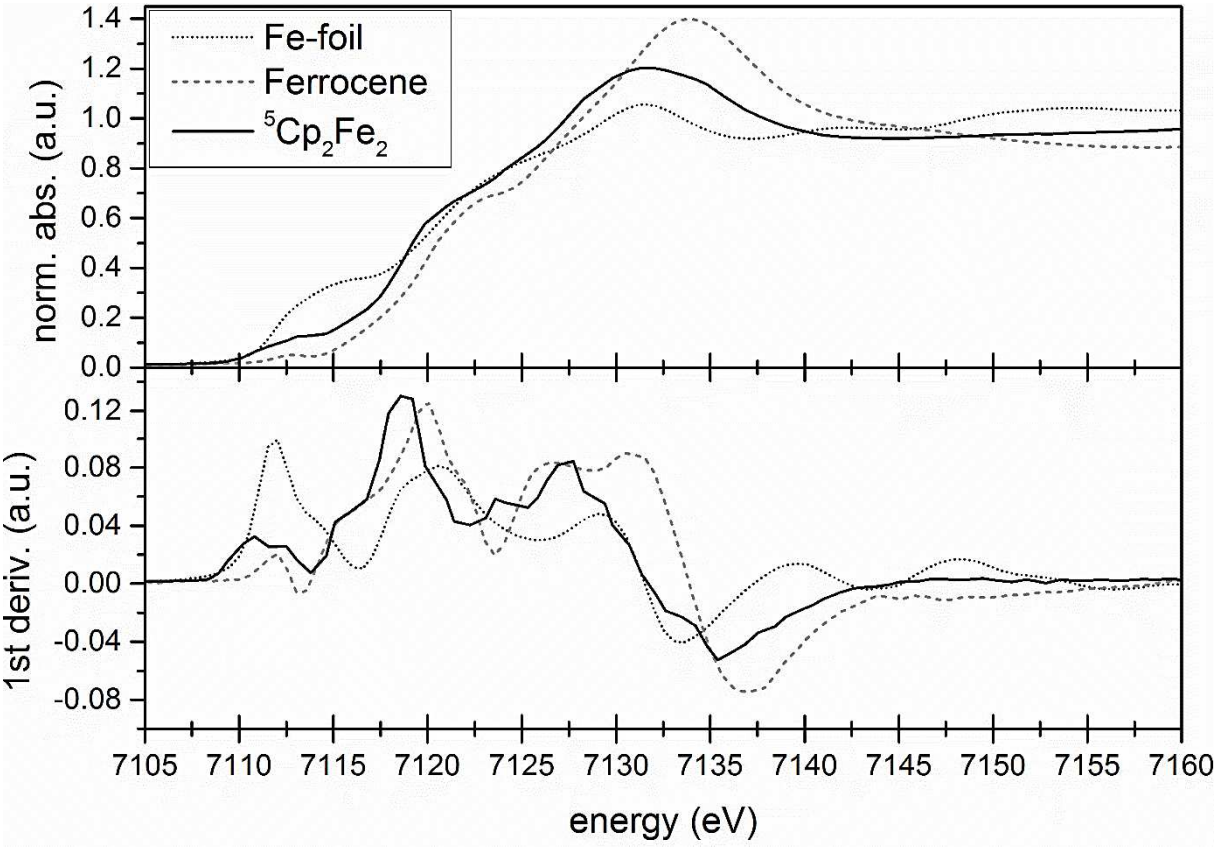

Figure 1: XAS spectrum of $^5Cp_2Fe_2$ (top) and the first derivative (bottom). Ferrocene and an iron foil are plotted as reference spectra.

The energy of the iron K-edge in $^5Cp_2Fe_2$ is determined at 7118.5 eV. With this the absorption edge of the complex lies between the absorption edges of the used references Fe^0 (7112.0 eV) and Fe^{+II} (7120.0 eV). The oxidation state is thus suspected to be an intermediate of these two values. Moreover, the edge position in $^5Cp_2Fe_2$ is identical to Fe^{+I}-species determined in an earlier study [1].It can therefore be concluded that in $^5Cp_2Fe_2$ iron is present as Fe(I).This conclusion is further backed by the prepeak at 7113.0 eV, attributed to a 1s-3d transition,[2] which is relatively broad. This indicates a metalloid character defined by low-valent metal-metal bonds. The shoulder at 7121.0 eV can be assigned to transitions from the 1s orbital of iron to π-orbitals of the conjugated cyclopentadienyl system[3].

Through evaluation of the extended X-ray absorption fine structure (EXAFS) range above the absorption edge) information can be obtained about the number of neighbour atoms, their type and their distances. In table 1 and figure 2 the fitting results and structural parameters of the analysis of $^5Cp_2Fe_2$ are shown. The obtained distances of all adjusted shells fit very well to the distances received from single crystal diffraction. In the first shell 4.9 carbon atoms could be fitted in a distance of 2.092 Å, which reflect very well the coordination of the cyclopentadienyl system. The tertiary carbon atoms of the isopropyl residues of the cyclopentadienyl system could be adjusted in a distance of 3.313 Å from the absorbing iron atom and one half of the methyl carbon atoms at 3.582 Å. Due to the similar distances, the other half of the methyl atoms are represented in the shell at 4.318 Å mixed with carbon atoms of the second cyclopentadienyl system, coordinating to the second iron atom. The unrealistic numbers of carbon atoms in the shells at 3.313 Å, 3.582 Å and 4.318 Å can be

explained with the low atom weight and the relatively big distances to the absorbing atom.[4] The fitted iron-iron distance of 2.256 Å is shorter than the iron distance in bulk metal of 2.482 Å and supports therefore the assumption of iron with the oxidation state of +I in the complex.

Table 1: EXAFS analysis fitting parameters and results of the spectrum of $^5Cp_2Fe_2$				
Abs-Bs[a)]	N(Bs)[b)]	R(Abs-Bs)/Å[c)]	σ/Å^{-1} [d)]	R/%[e)] χ^2_{red} [f)] E_f/eV[g)] Afac[h)]
Fe-C	4.9±0.4	2.092±0.020	0.059±0.005	34.05
Fe-Fe	1.2±0.1	2.256±0.022	0.087±0.008	26.4558E-6
Fe-C	8.1±0.8	3.313±0.033	0.112±0.011	5.006
Fe-C	2.2±0.2	3.582±0.035	0.032±0.003	0.4846
Fe-C	2.6±0.2	4.318±0.043	0.045±0.004	
a) Abs=X-ray absorbing atom, BS=backscattering atom, b) number of backscattering atoms, c) distance between absorbing and backscattering atom, d) Debye-Waller-like factor, e) fit index, f) reduced χ^2 error (considers beside error to experiment the number of independent points and number of varied parameters), g) Fermi energy, that account for the shift between theory and experiment, h) amplitude reducing factor				

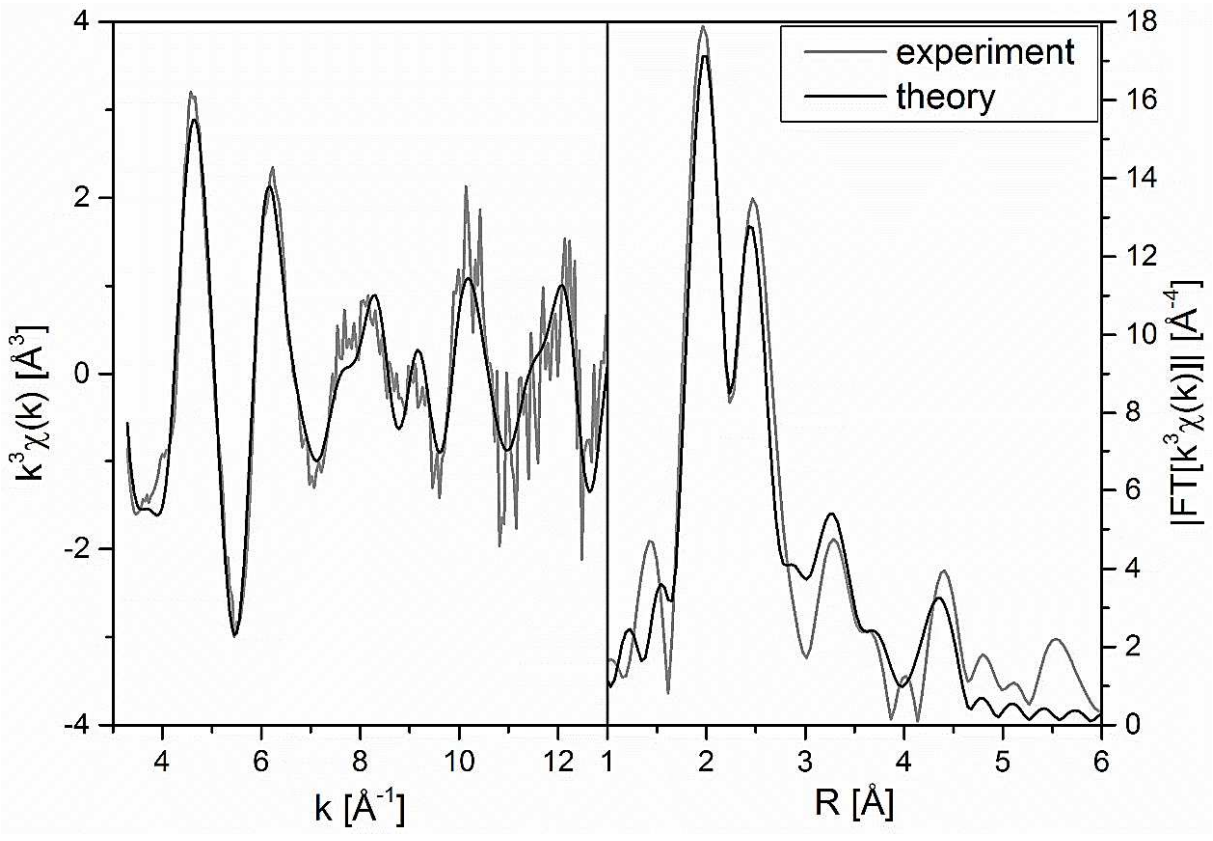

Figure 2: EXAFS analysis with k³χ(k) (left) and the corresponding Fourier transformed in R-space (right).

ESI

Data analysis

In the first step of data analysis the background of the spectrum was removed by subtracting a Victoreen-type polynomial[5]. Due to the very differing shapes of the absorption edges of the samples and the used references, the first inflection point of the first derivative of the corresponding spectrum was defined as energy E_0. Afterwards a piecewise polynomial was used to determine the smooth part of the spectrum and was adjusted in a way that the low-R components of the resulting Fourier transform were minimal. The background subtracted spectrum was divided by its smoothed part and the photon energy was converted to photoelectron wave number *k*. For evaluation of the EXAFS spectra the resulting functions were weighted with k^3 and calculated with EXCURVE98, which works based on the EXAFS function and according to a formulation in terms of radial distribution functions[6]:

$$\chi(k) = \sum_j S_0^2(k) F_j(k) \int P_j(r_j) \frac{e^{\frac{-2r_j}{\lambda}}}{kr_j^2} \sin\left[2kr_j + \delta_j(k)\right] dr_j$$

The number of independent points N_{ind} was calculated according to information theory to determine the degree of overdeterminacy[6b]:

$$N_{ind} = \frac{2\Delta k \Delta R}{\pi}$$

Here, *Δk* describes the range in *k*-space used for data analysis and *ΔR* corresponds to the distance range in the Fourier filtering process. For the analysis a *Δk*-range of 10 and a *ΔR*-range of 3 was used, which yielded a number of independent points of 19.1. The quality of a fit was determined using two methods. The reduced χ^2_{red} considers the degree of overdeterminacy of the system and the number of fitted parameters *p*. It therefore allows a direct comparison of different models[7]:

$$\chi^2_{red} = \frac{\left({}^{N_{ind}}/_{N}\right)}{N_{ind} - p} \sum_i \left(\frac{k_i^n}{\sum_j k_j^n \left| \chi_j^{exp}(k_j) \right|} \right)^2 \left(\chi^{exp}(k_i) - \chi^{theo}(k_i)\right)^2$$

The R-factor, which represents the percental disagreement between experiment and adjusted function and takes into account both systematic and random errors according to the equation[7]:

$$R = \sum_i \frac{k_i^n}{\sum_j k_j^n \left| \chi_j^{exp}(k_j) \right|} \left| \chi^{exp}(k_i) - \chi^{theo}(k_i) \right| \cdot 100\%$$

The accuracy of the determined distances is 1 %, of the Debye-Waller-like factor 10 %[8] and of the coordination numbers depending of the distance 5-15 %. The amplitude reducing factor was iterated free in every fit.

Literature

[1] R. Schoch, W. Desens, T. Werner and M. Bauer, *Chem. Eur. J.* **2013**, *19*, 15816-15821.
[2] a) M. Bauer and C. Gastl, *Phys. Chem. Chem. Phys.* **2010**, *12*, 5575-5584; b) M. Bauer, T. Kauf, J. Christoffers and H. Bertagnolli, *Phys. Chem. Chem. Phys.* **2005**, *7*, 2664-2670.
[3] K. S. M. Salih, S. Bergner, H. Kelm, Y. Sun, A. Grün, Y. Schmitt, R. Schoch, M. Busch, N. Deibel, S. Bräse, B. Sarkar, M. Bauer, M. Gerhards and W. R. Thiel, *Eur. J. Inorg. Chem.* **2013**, 6049-6059.
[4] M. Bauer, S. Müller, G. Kickelbick and H. Bertagnolli, *New J. Chem.* **2007**, *31*, 1950-1959.
[5] a) T. S. Ertel, H. Bertagnolli, S. Hückmann, U. Kolb and D. Peter, *Appl. Spectrosc.* **1992**, *46*, 690-698; b) M. Newville, *J. Synchrotron Rad.* **2001**, *8*, 322-324; c) M. Newville, P. Livins, Y. Yacoby, J. J. Rehr and E. A. Stern, *Phys. Rev. B* **1993**, *47*, 14126-14131; d) B. Ravel and M. Newville, *J. Synchrotron Rad.* **2005**, *12*, 537-541.
[6] a) N. Binsted and S. S. Hasnain, *J. Synchrotron. Radiat.* **1996**, *3*, 185-196; b) N. Binsted and F. Mosselmans, *EXCURV98 Manual*, Daresbury, UK, p.
[7] M. Bauer and H. Bertagnolli, *J. Phys. Chem. B* **2007**, *111*, 13756-13764.
[8] D. C. Koningsberger, B. L. Mojet, G. E. van Dorssen and D. E. Ramaker, *Top. Catal.* **2000**, *10*, 143-155.

$(^5CpFeH_2)_2$ (12)

^{1}H-NMR

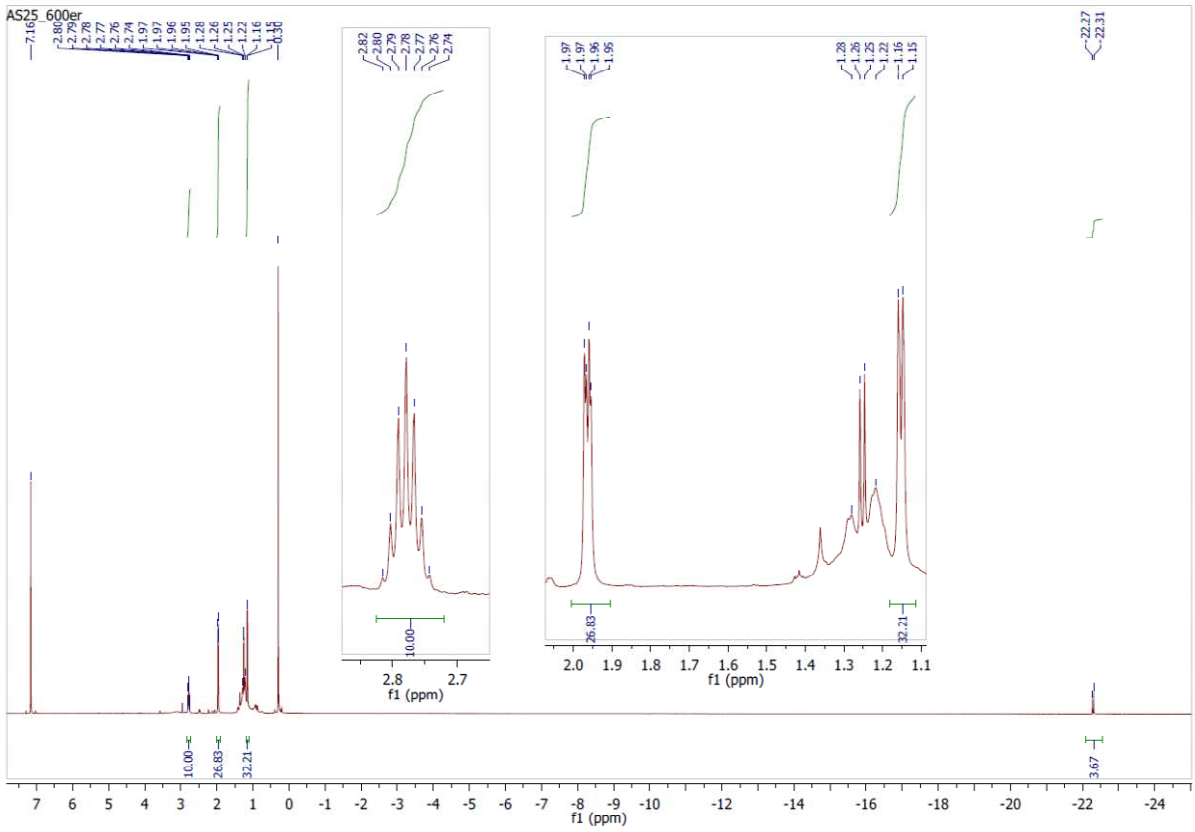

$(^5CpFeN)_2$ (7)

^{1}H-NMR

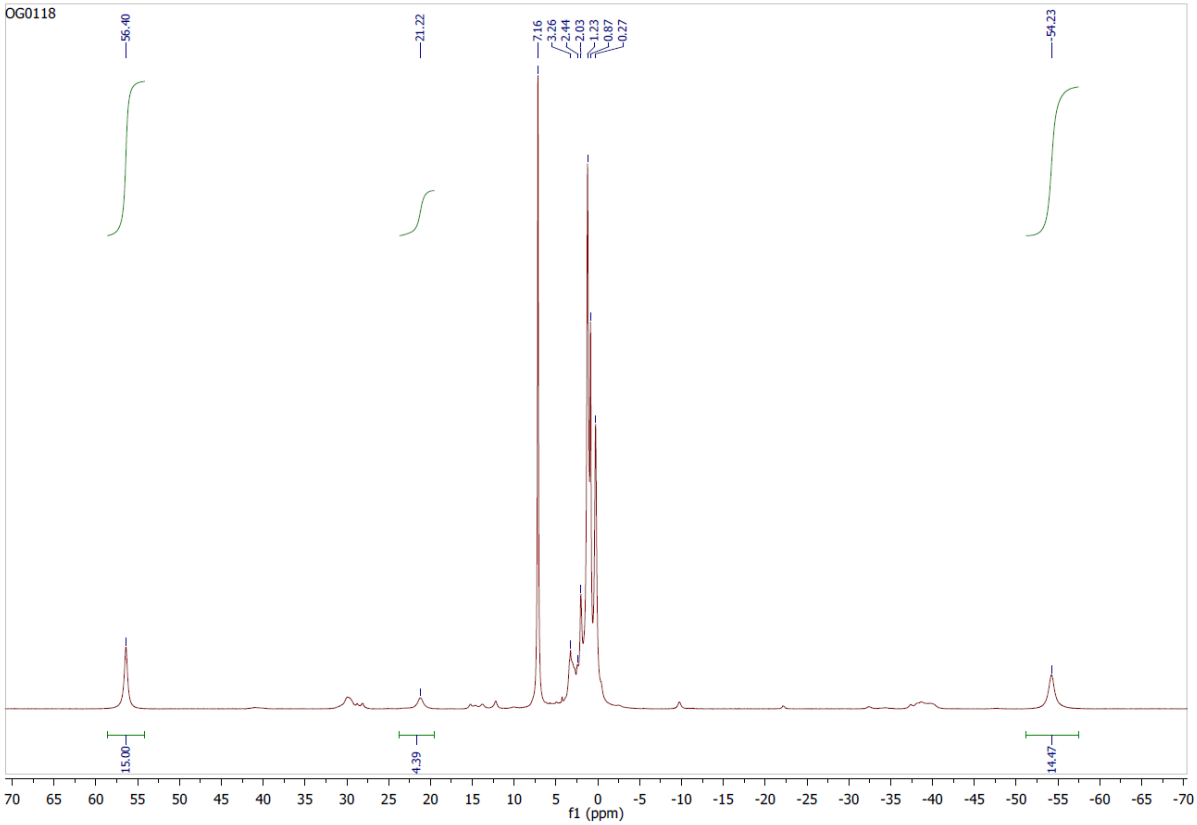

$(C_5Me_5)FeBr(TMEDA)$ (13)

^{1}H-NMR

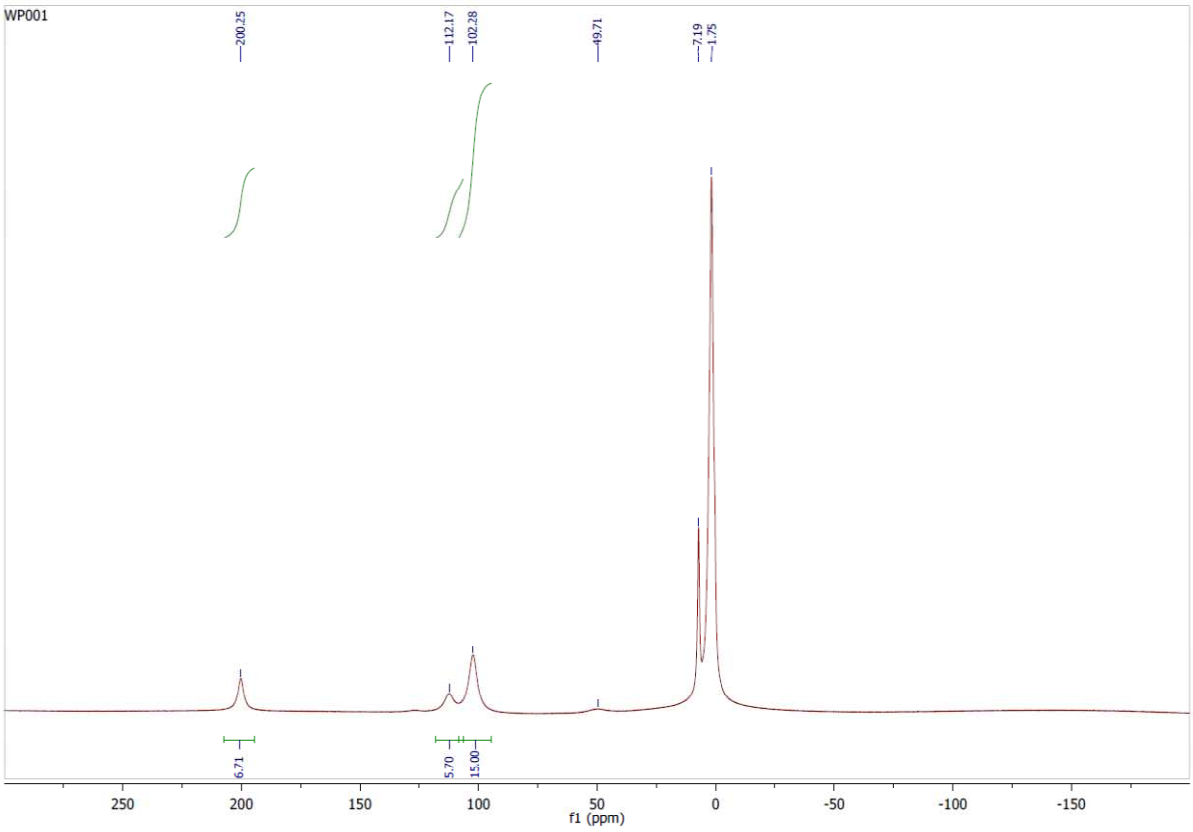

2,5-Dimethyl-3,4-(1-ethylpropyl)cyclopenta-2-en-1-on

^{1}H-NMR

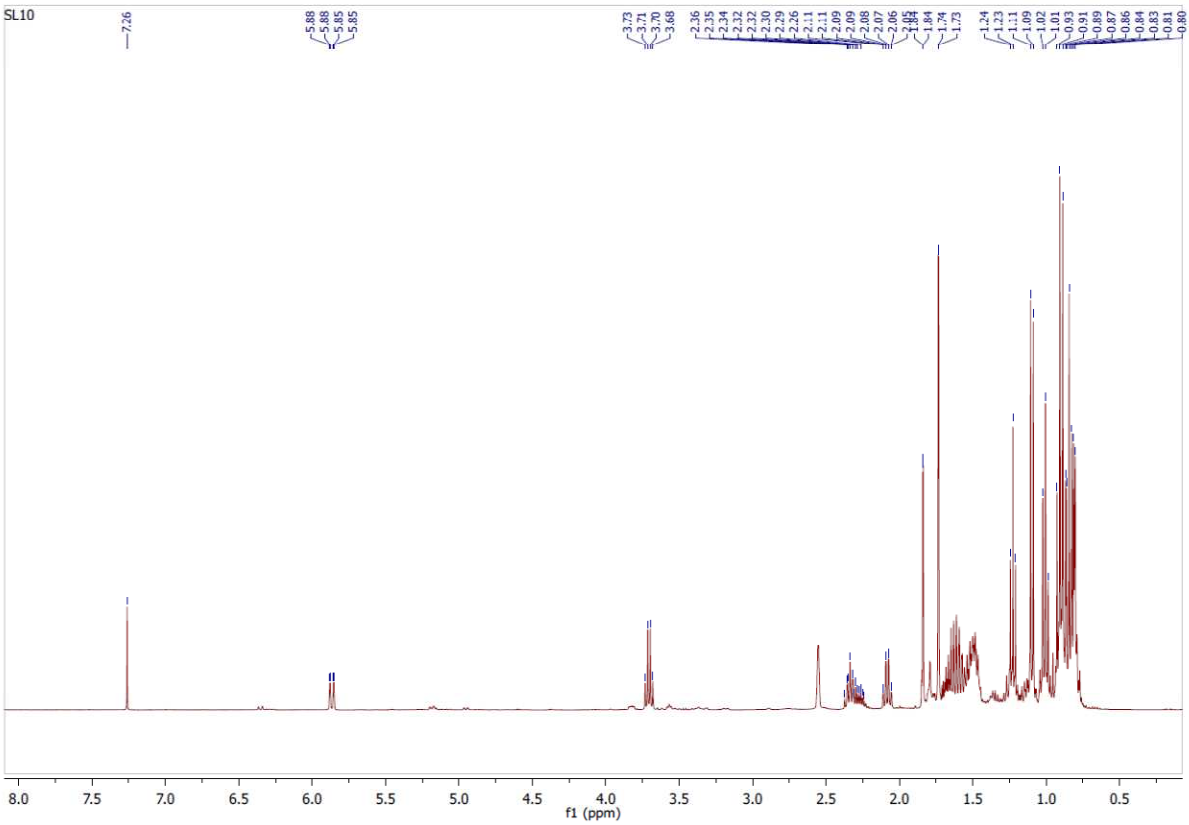

^{13}C-NMR

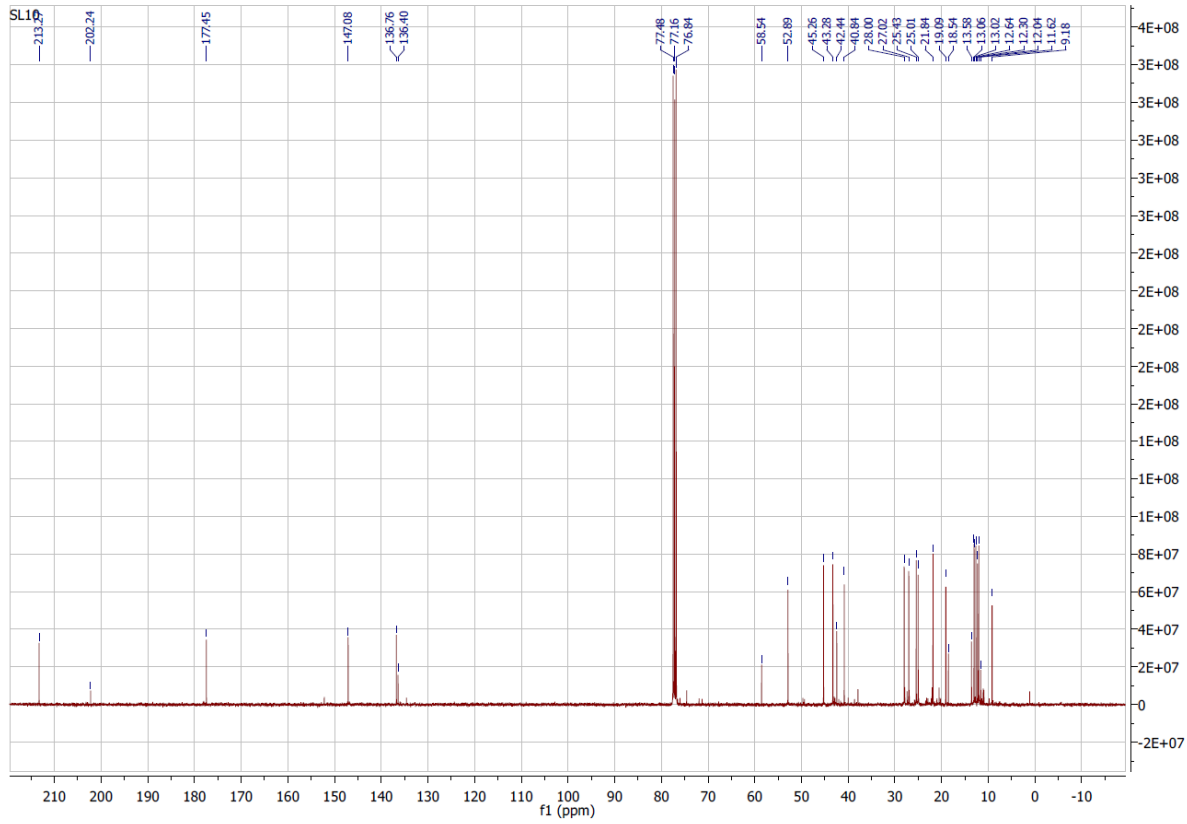

4,6-Diisopropyl-2,8-Dimethyl-nona-3,6-dien-5-on (3)

^{1}H-NMR

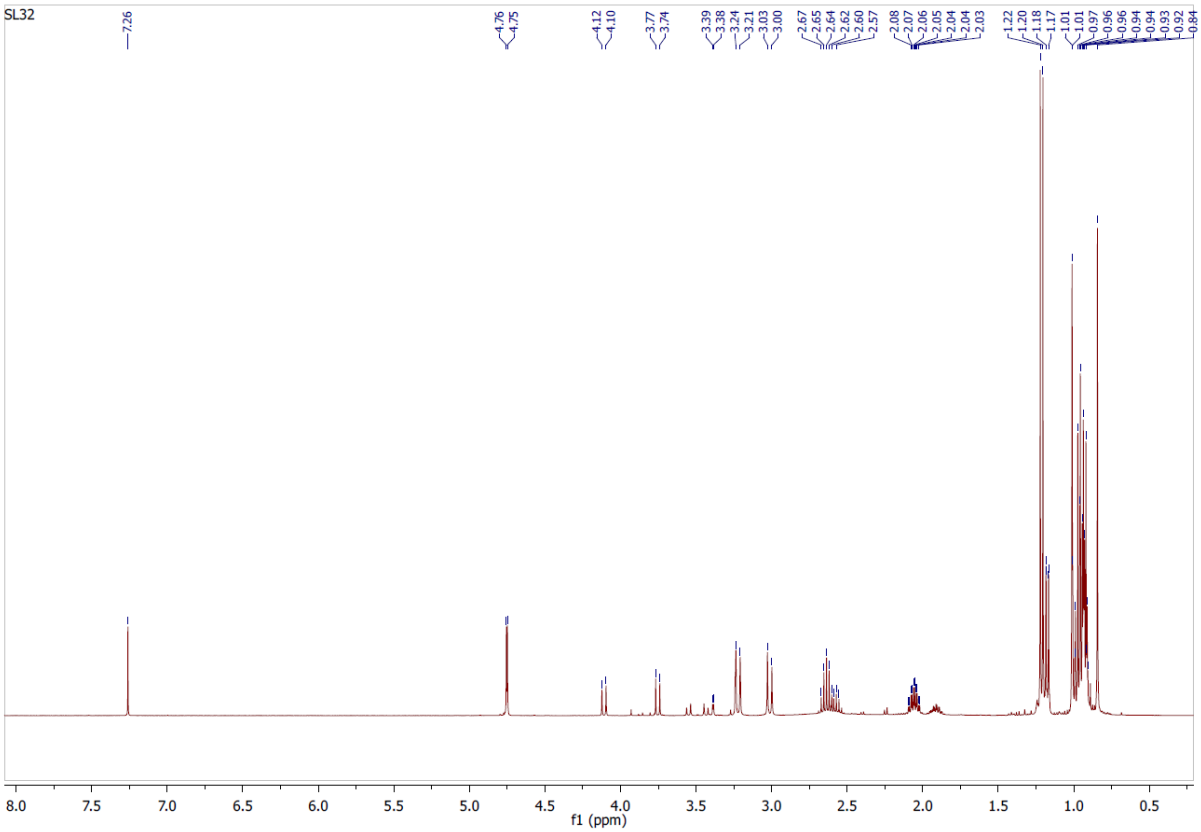

HHCOSY

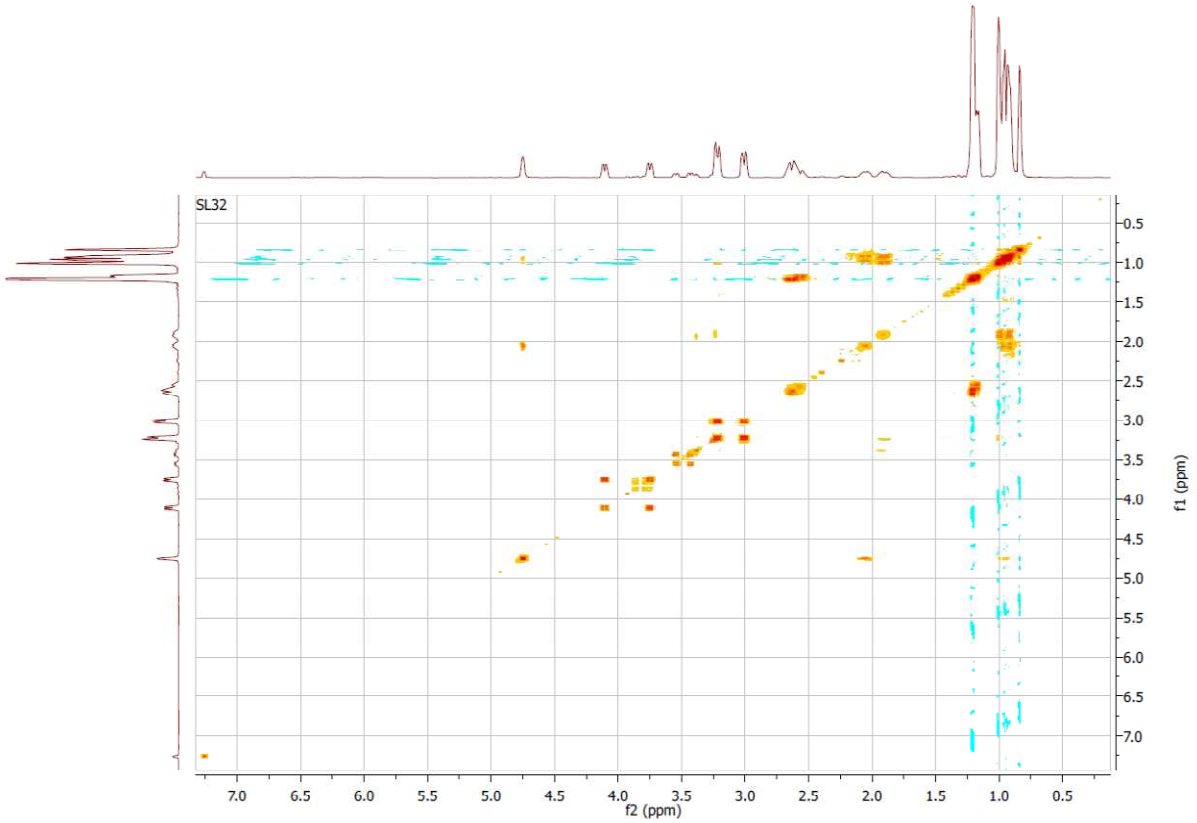

hmqc

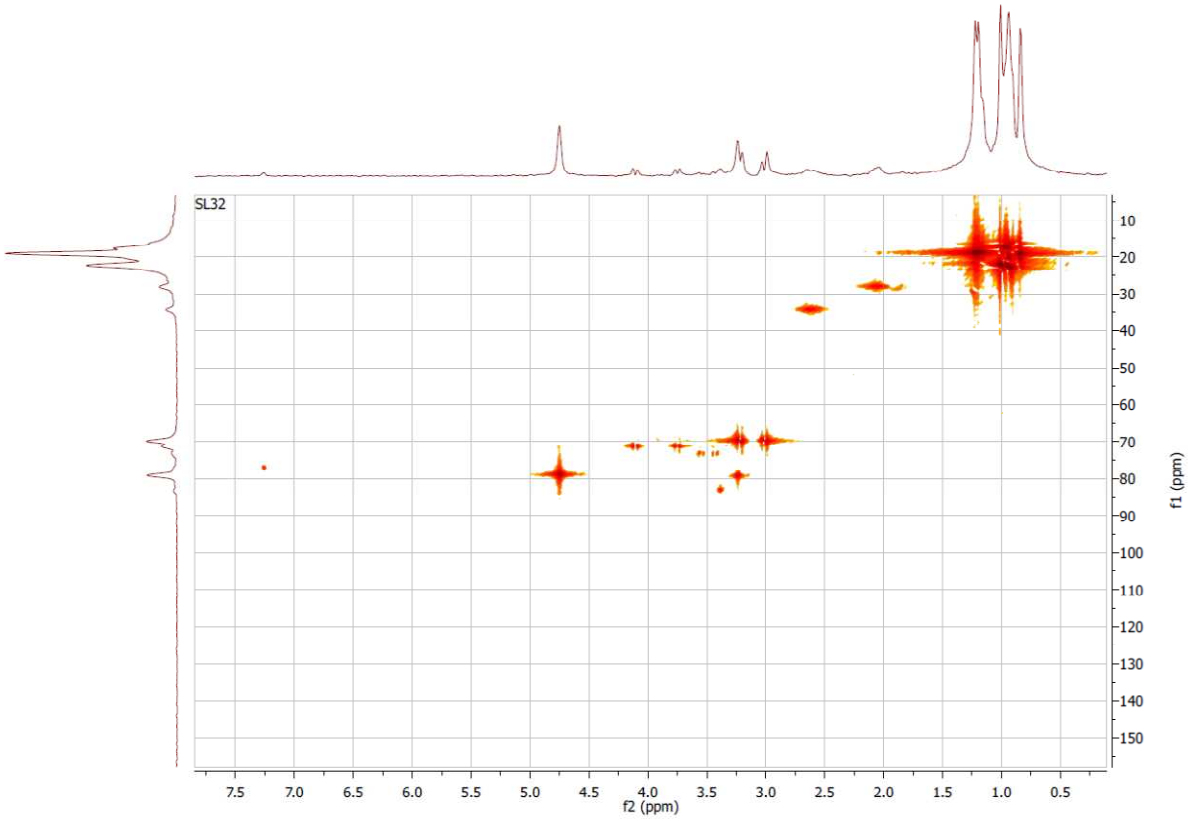
SL32
10
20
30
40
50
60
70
80
90
100
110
120
130
140
150
f1 (ppm)
7.5
7.0
6.5
6.0
5.5
5.0
4.5
4.0
3.5
3.0
2.5
2.0
1.5
1.0
0.5
f2 (ppm)

$^{5}CpFeH(HPPh_2)_2$ (22)

^{1}H-NMR

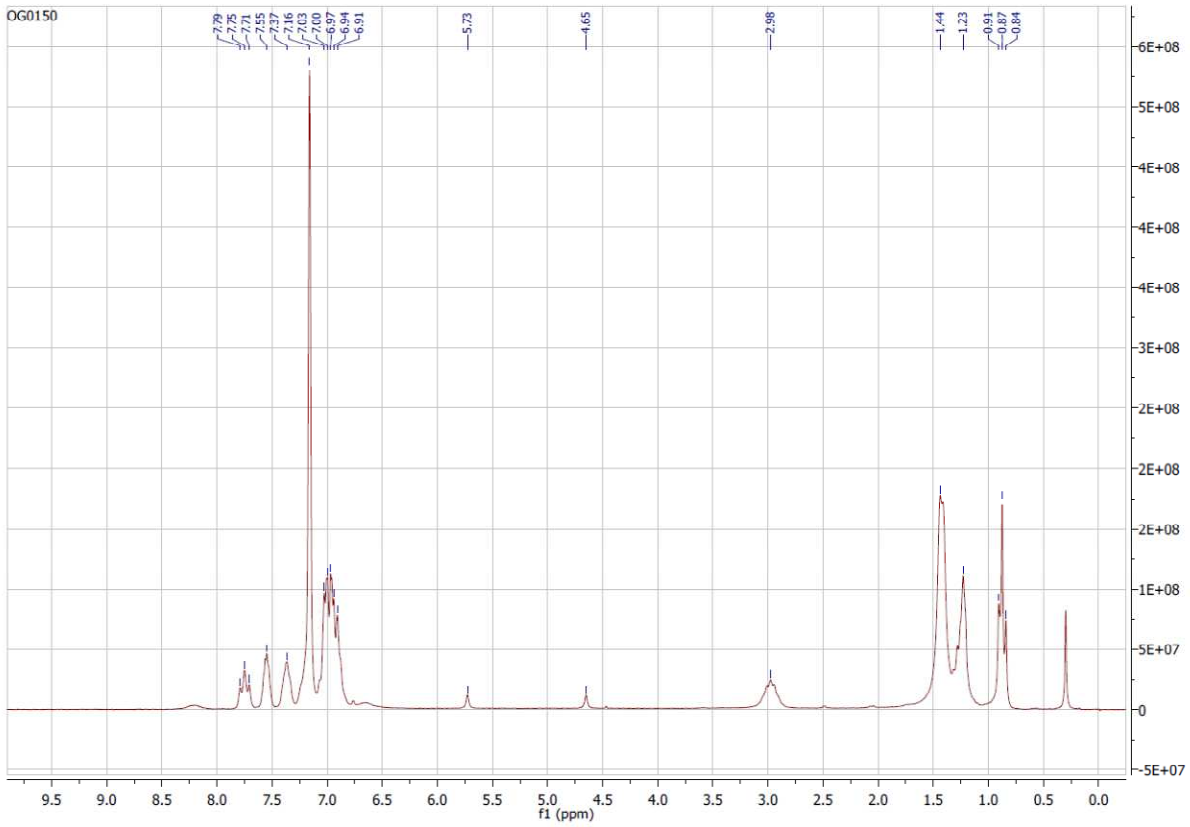

$^{5}CpFeN(SiMe_3)_2$ (16)

^{1}H-NMR